A NEW DIGITAL LOW-LEVEL RF AND LONGITUDINAL DIAGNOSTIC SYSTEM FOR CERN'S AD

M. E. Angoletta[†], S. C. P. Albright, M. Jaussi, A. Findlay, V. R. Myklebust, J. C. Molendijk, CERN, Geneva, Switzerland

Abstract

The Antiproton Decelerator (AD) has been routinely providing 3 E7 antiprotons since July 2000 at 100 MeV/c from 3.5 GeV/c. It will be refurbished during the Long Shutdown 2 (LS2) to provide reliable operation for the new Extra Low ENergy Antiproton (ELENA) ring. AD will be equipped with a new digital Low-Level RF (LLRF) system before its restart in 2021. Diagnostics to measure beam intensity, $\Delta p/p$ and Schottky spectra will also be developed. This paper is an overview of the planned capabilities and implementations, as well as of the challenges to overcome.

INTRODUCTION

In operation since July 2000 [1], CERN's Antiproton Decelerator (AD) provides the physics program with low-energy antiprotons by decelerating 3 E7 particles per cycle to 5.3 MeV kinetic energy. It will be upgraded and consolidated [2] during the Long Shutdown 2 (LS2) to provide reliable operation to the Extra Low ENergy Antiproton (ELENA) ring [3]. Changes to the AD include replacing its decelerating, ferrite-based High-Level RF (HLRF) system with one based on Finemet metal alloy. A new Low-Level RF (LLRF) with additional functionalities will control it. The existing longitudinal intensity and Schottky measurement system will also be upgraded.

Table 1 shows the momentum and revolution frequency values at each flattop. Figure 1 shows the typical AD production cycle including the RF segments, i.e. cycle parts where the RF is active. Energy levels and cycle structure will not change after LS2.

Table 1: AD Flattop Momentum and Frequency Values

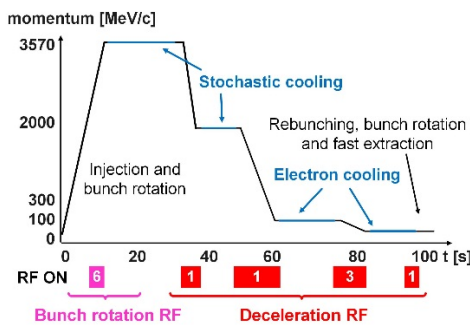| Flattop	Momentum	Revolution frequency
FT1	3.57 GeV/c	1.589478 MHz
FT2	2 GeV/c	1.487728 MHz
FT3	300 MeV/c	500.465 kHz
FT4	100 MeV/c	174.155 kHz

Figure 1: AD production cycle.

†maria.elena.angoletta@cern.ch

LOW-LEVEL RF SYSTEM

Hardware and Software

The AD LLRF system belongs to the same hardware and software family already deployed in several CERN machines [4 - 7]; it will be a modified version of that successfully deployed in ELENA [6, 7].

Figure 2 shows a schematic view of the system. Two boards will interact in real time to carry out the requested tasks. The FPGA Mezzanine Card (FMC) [8] daughter-cards will be clocked by a fixed 122.7 MHz clock. This is the new standard for the LLRF family and allows Analogue-to-Digital and Digital-to-Analogue converters to operate with an optimal signal-to-noise ratio. The challenge of tracking bunches over a wide frequency swing will be addressed by sophisticated FPGA filters.

Inputs will come from a Longitudinal Pick-Up (LPU) [9] and from a Transverse Pick-up (TPU). The LLRF will be interfaced to the orbit system [10] via optical fibres, to send the revolution frequency and to get the measured orbit. The magnetic field value will be obtained via optical fibre [11]. The LLRF will control the HLRF system, as detailed later.

The LLRF will generate several RF trains. The h = 1 train will be sent to the analogue data acquisition and to the tomoscope [12] systems. The LLRF will give harmonic number, detected voltage, Btrain value and Btrain derivative to the tomoscope. An h = hRF train will be sent to the timing and an h = 8 train to the tune measurement systems.

System Capabilities and Operation

The frequency program is implemented from a synthetic (not measured) Btrain. The beam phase loop will receive signals from the LPU and will damp coherent longitudinal dipole oscillations. A radial loop, absent in the previous LLRF, will be deployed. This will correct frequency errors caused by the synthetic Btrain; its input will be user-selectable: TPU or orbit signals. The extraction synchronisation loop will lock the bunch to an external reference, improving the extracted bunch energy reproducibility.

As the AD cycle lasts nearly two minutes, diagnostics data will need to be published before it ends. The beam is bunched/debunched in each RF segment; the 1024 vectors in each LLRF function will allow covering the whole cycle. Settings will be integrated in the AD RF cycle editor and will be automatically adapted to cycle length changes. Finally "PAUSES", where the execution of the magnetic cycle is stopped, will be managed by the LLRF system. Antiproton stacking and extraction at 300 MeV/c, not planned after LS2, will not be included in the LLRF. It will be possible to add these features later on.

MC6: Beam Instrumentation, Controls, Feedback and Operational Aspects
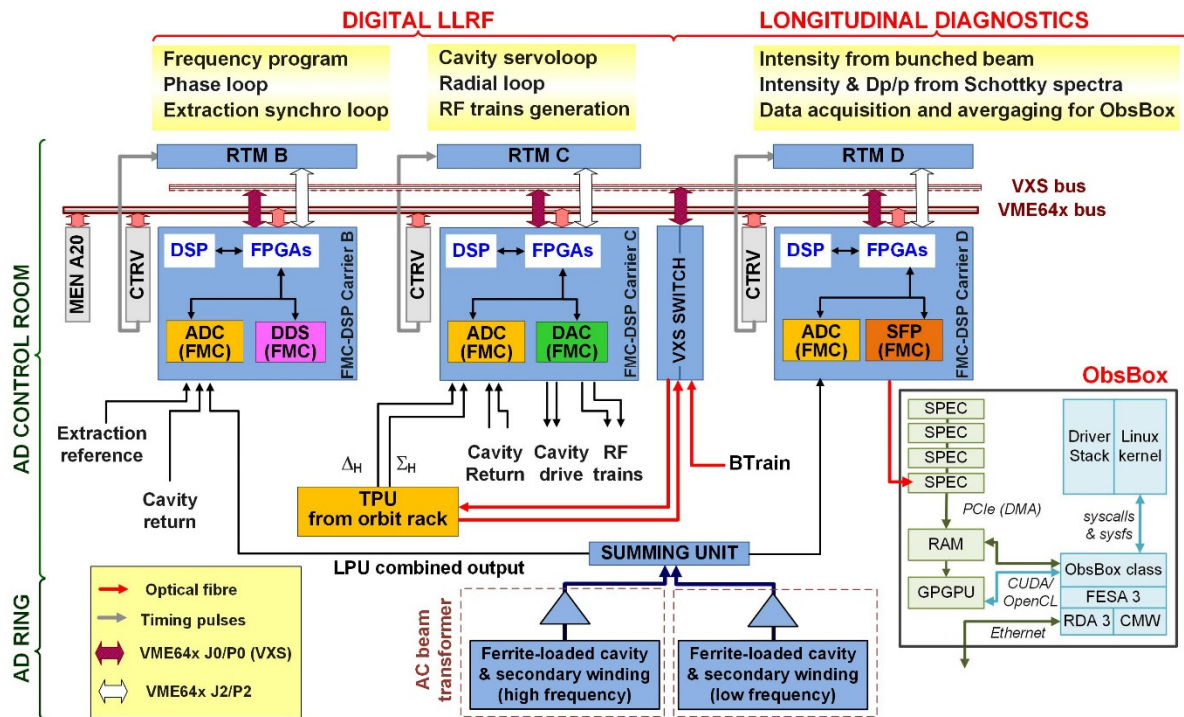
T27 Low Level RF

Figure 2: AD LLRF and longitudinal diagnostics. Keys: DDS –Direct Digital Synthesiser, ADC – Analogue-to-Digital Converter, DAC – Digital-to-Analogue Converter, SFP – Small Form-factor Pluggable Transceiver, LPU/TPU – Longitudinal/Transverse Pick-Up, CTRV – Timing Receiver Module, MEN A20 – Master VME board, RTM – Rear Transition Module, ObsBox – custom acquisition/processing module, SPEC – Simple PCI Express carrier module.

Operation of the HLRF System

The wide-band, non-tuneable HLRF system will be based on a Finemet metal alloy. Table 2 shows the available voltage as a function of frequency. Typically 3 kV are needed for deceleration and 500 V at extraction. Operation at $h = 3$ will be required on the third ramp, similarly to what was done with the previous HLRF.

Table 2: HLRF Voltage as a Function of Frequency

Frequency range [kHz]	Max Voltage [Vpeak]
145 – 500	500
500 - 2000	3500
Elsewhere	0

Voltage and phase loop for a single decelerating harmonic will be implemented by the LLRF in [I, Q] coordinates. The impact of the new Finemet cavity has been investigated with numerical calculations and longitudinal tracking in the BLonD code [13]. A higher-than-operational intensity of 1 E8 antiprotons and low longitudinal emittance of 1eVs was used to look beyond expected demands on the system. The induced voltage caused by the Finemet impedance is expected to be of the order of 1 Volt; tracking simulations show no impact on beam stability. Figure 3 shows a side-by-side comparison of phase space at the start and end of the first ramp.

The LLRF will control in real time the gap relay short-circuiting the HLRF when no voltage is required. Safeguards in the LLRF will prevent overdriving the HLRF and remove the drive signal if the HLRF is not ready.

A sophisticated mechanism will measure the HLRF transfer function during setting-up, compensate for its frequency nonlinearity and cope with the frequency sweep.
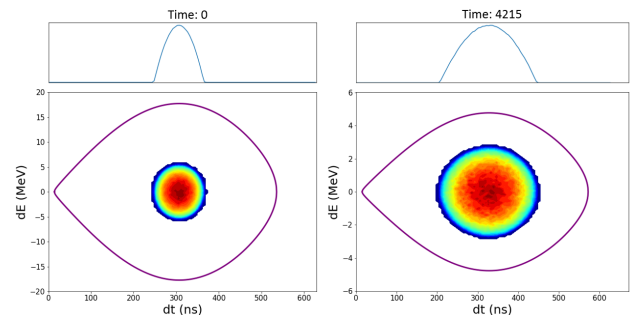

Figure 3: Phase space simulation for the first ramp beginning (left) and end (right).

LONGITUDINAL DIAGNOSTIC SYSTEM

Introduction

Standard DC beam transformers do not operate at AD's low beam intensities. Since its start, AD was thus equipped with a dedicated longitudinal diagnostics system [14, 15] processing data from a low noise LPU [9]. The system, strictly linked to the LLRF, measured the intensity NP for a bunched beam by Fourier analysis; Schottky spectra, NP and Δp/p were also provided for debunched beams. The system was instrumental for operating and optimising the machine. Figure 4 shows the performance summary table available at the end of each cycle. Figure 5 shows the plot of measured NP, Δp/p and revolution frequency.
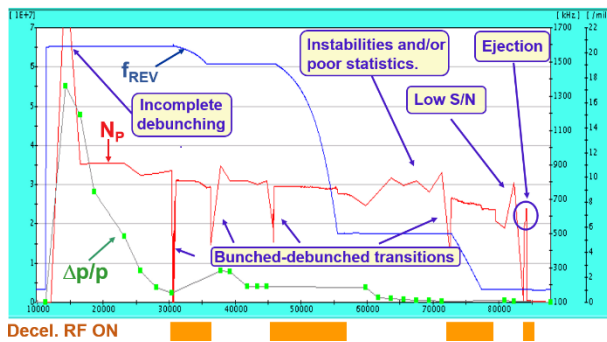
Figure 4: Cycle performance - summary table.

Figure 5: Longitudinal diagnostics plot for an AD cycle.

A new longitudinal measurement system will be developed for AD's restart in 2021. Figure 2 shows the two main system components: the FMC-DSP-Carrier board D and a fast processing module ("ObsBox") receiving data from it via optical fibre. The new system will provide not only performance monitoring data for machine operators but also advanced information for cooling experts.

Data Processing in Frequency

The FMC-DSP-Carrier board D, shown in Figure 2, will process downconverted data derived from the LPU.

For bunched beams, bunch length and N_P will be calculated with the method used in the previous system [14]. These measurements were already successfully deployed for ELENA [7]. Figure 6 shows how bunched beam parameters are derived from two Fourier components, assuming a parabolic envelope. Dependence on bunch shape is a drawback of this method.
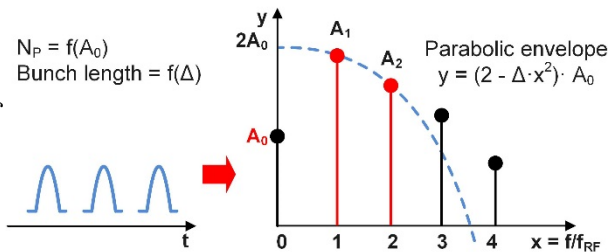

Figure 6: Bunched beam processing in frequency.

Debunched beam data will also be processed and complex FFTs averaging will be used. Outputs will be spectra, N_P, $\Delta p/p$ and f_{REV} deviation from the nominal value. FFT sizes of 512 and 1024 will be available.

Bunched and debunched beam data will be available during the cycle. They will be published as standard virtual scope signals, thus allowing the operators to correlate their variations with other phenomena in the machine.

Data Processing in Time

The processing of longitudinal data in time will be carried out by the ObsBox, shown in Figure 2. This is a custom acquisition/processing system and a standard CERN RF building block, already deployed in other machines [16]. It has a fast computer, fully integrated in and supported by CERN's controls infrastructure, with deep memory and high processing power. It hosts a Linux server running real-time software to perform online data analysis. Clients connect directly to the ObsBox via Ethernet.

The ADC FMC on the FMC-DSP-Carrier board D will sample longitudinal signals at 122.7 MHz and average pairs of samples to obtain data at 61 MHz. This data stream will then be packed in frames containing the revolution frequency value and the bunched/debunched beam status; the FMC-DSP-Carrier board D will have access to these data as hosted in the LLRF crate. The data stream will be sent to the ObsBox by a commercial SFP FMC over an optical fibre running at 2 Gb/s (corresponding to 100 MSPS). We are evaluating higher data transfers that would enable sending data sampled at the full rate. A circular buffer in the ObsBox will store data for several AD cycles.

For bunched beams, bunch integration and baseline subtraction will be used, removing the bunch shape dependence inherent on frequency processing. Sampling the data at 61 MHz allows about 10 samples/bunch even for the shortest bunches. Bunch length and NP will be provided.

For debunched beams, high-length FFTs will deliver good frequency resolution. The numerical values of NP and of $\Delta p/p$ at specific points in the cycle will allow evaluating machine performance. Waterfall plots of spectra will be available for cooling experts.

OUTLOOK AND CONCLUSIONS

AD will restart operating in 2021 equipped with new LLRF and longitudinal diagnostics. The layout of the two combined systems will be validated in the 2020 ELENA run. Many LLRF and diagnostics features have already been deployed in ELENA and the remaining ones, such as the ObsBox integration, will be validated in 2020.

AD will profit from synergy with other machines for essential building blocks, such as the fixed frequency clocking scheme, operation with the new Btrain distribution system, operation with RF segments and integration of settings within an RF cycle editor. In turn, other machines will profit from features deployed in the AD system. An example is the PSB LLRF [17] where adding the ObsBox will allow measuring the bunch length along the cycle.

REFERENCES

[1] P. Belochitskii *et al*., "Commissioning and First Operation of the Antiproton Decelerator AD", in *Proc. PAC '01*, Chicago, Illinois, USA, June 2001, pp. 580 – 584.

[2] T. Eriksson *et al*., "Upgrades and Consolidation of the CERN AD for Operation During the Next Decades", in *Proc. IPAC'13*, Shanghai, China, May 2013, pp. 2654 – 2656.

[3] T. Eriksson *et al*., "ELENA – From Installation to Commissioning", *in Proc. IPAC '17*, Copenhagen, Denmark, May 2017, pp. 3327 – 3330.

[4] M. E. Angoletta *at al*., "The new LEIR Digital Low-Level RF system", *in Proc. IPAC '17*, Copenhagen, Denmark, May 2017, pp. 4062 – 4065.

[5] M. E. Angoletta *et al*., "Operational Experience with the New Digital Low-Level RF System for CERN's PS Booster", in *Proc. IPAC '17*, Copenhagen, Denmark, May 2017, pp. 4058 – 4061.

[6] M.E. Angoletta et al, "Initial Beam Results of CERN ELENA's Digital Low-Level RF System", in *Proc. IPAC '17*, Copenhagen, Denmark, May 2017, pp. 4054 – 4057.

[7] M. E. Angoletta. M. Jaussi, J. C. Molendijk, "The New Digital Low-Level RF System for CERN's Extra Low ENergy Antiproton machine", presented at IPAC'19, Melbourne, Australia, May 2019, paper THPRB069, this conference.

[8] ANSI/VITA 57.1 standard

[9] F. Pedersen, C. Gonzalez, "An Ultra Low Noise AC Beam Transformer for Deceleration and Diagnostics of Low Intensity Beams", in *Proc. PAC '99*, New York, USA, 1999, pp. 474-476.

[10] R. Marco-Hernandez *at al*., "A New Orbit System for the CERN Antiproton Decelerator", in *Proc. IBIC2015*, Melbourne, Australia, September 2015, pp. 465 – 469.

[11] P.P.M. Jansweijer, H.Z. Peek, E. de Wolf, "White Rabbit: Sub-nanosecond timing over Ethernet", Nuclear Instruments and Methods in Physics Research A 725 (2013), pp. 187 – 190.

[12] http://tomograp.home.cern.ch

[13] CERN Beam Longitudinal Dynamics code BLonD http://blond.web.cern.ch

[14] M. E. Angoletta, V. Chohan, M. Ludwig, O. Marqversen, F. Pedersen, "The New Digital-Receiver-Based System for Antiproton Beam Diagnostics", in *Proc. PAC '01*, Chicago, Illinois, USA, June 2001, pp. 2371 – 2373.

[15] M. E. Angoletta *et al*., "Upgrades to the Digital Receiver-Based Low-Intensity beam Diagnostics for CERN AD", The New Digital-Receiver-Based System for Antiproton Beam Diagnostics", in *Proc. PAC '03*, Portland, Oregon, USA, May 2003, pp. 2461 – 2463.

[16] M. Ojeda *et al*., "Processing High-Bandwidth Bunch-by-Bunch Observation Data from the RF and Transverse Damper Systems of the LHC", in *Proc. ICAPEPCS2015*, Melbourne, Australia, October 2015, pp. 841 – 844.

[17] M. E. Angoletta, S. C. P. Albright, A. Findlay, M. Jaussi, J. C. Molendijk, and N. Pittet, "Upgrade of CERN's PSB Digital Low-Level RF System", presented at the 10th Int. Particle Accelerator Conf. (IPAC'19), Melbourne, Australia, May 2019, paper THPRB068, this conference.